

# Gill Morphometrics in Relation to Gas Transfer and Ram Ventilation in High-Energy Demand Teleosts: Scombrids and Billfishes

Nicholas C. Wegner,<sup>1\*</sup> Chugey A. Sepulveda,<sup>2</sup> Kristina B. Bull,<sup>1</sup> and Jeffrey B. Graham<sup>1</sup>

<sup>1</sup>Center for Marine Biotechnology and Biomedicine, Marine Biology Research Division, Scripps Institution of Oceanography, University of California San Diego, La Jolla, California 92093

<sup>2</sup>Pfleger Institute of Environmental Research, Oceanside, California 92054

**ABSTRACT** This comparative study of the gill morphometrics in scombrids (tunas, bonitos, and mackerels) and billfishes (marlins, swordfish) examines features of gill design related to high rates of gas transfer and the high-pressure branchial flow associated with fast, continuous swimming. Tunas have the largest relative gill surface areas of any fish group, and although the gill areas of non-tuna scombrids and billfishes are smaller than those of tunas, they are also disproportionately larger than those of most other teleosts. The morphometric features contributing to the large gill surface areas of these high-energy demand teleosts include: 1) a relative increase in the number and length of gill filaments that have, 2) a high lamellar frequency (i.e., the number of lamellae per length of filament), and 3) lamellae that are long and low in profile (height), which allows a greater number of filaments to be tightly packed into the branchial cavity. Augmentation of gill area through these morphometric changes represents a departure from the general mechanism of area enhancement utilized by most teleosts, which lengthen filaments and increase the size of the lamellae. The gill design of scombrids and billfishes reflects the combined requirements for ram ventilation and elevated energetic demands. The high lamellar frequencies and long lamellae increase branchial resistance to water flow which slows and streamlines the ram ventilatory stream. In general, scombrid and billfish gill surface areas correlate with metabolic requirements and this character may serve to predict the energetic demands of fish species for which direct measurement is not possible. The branching of the gill filaments documented for the swordfish in this study appears to increase its gill surface area above that of other billfishes and may allow it to penetrate oxygen-poor waters at depth. *J. Morphol.* 271:36–49, 2010. © 2009 Wiley-Liss, Inc.

**KEY WORDS:** gill surface area; gill dimensions; filament; lamellae; tuna; swordfish

## INTRODUCTION

Fish gill structure varies in relation to activity level and habitat use. Correspondingly, fishes with high metabolic requirements or inhabiting hypoxic environments generally have gill specializations

facilitating gas transfer (Hughes, 1966, 1970; Hughes and Morgan, 1973; De Jager and Dekkers, 1975; Graham, 2006; Mandic et al., 2009). Gill dimensions, including the length and abundance of gill filaments, the number of respiratory lamellae on the filaments, and lamellar bilateral surface area, are altered by selective factors to augment gill surface area and increase oxygen uptake from the water. Research on gill morphology and ventilatory mechanics suggests that teleost gill morphometrics balance the optimization of gas exchange to meet metabolic demands with the limitation of branchial resistance to minimize the energetic costs associated with the biphasic buccal-branchial pump system used to actively ventilate the gills (Hughes, 1966; Hughes and Morgan, 1973). Accordingly, Hughes (1966) theorized that gill surface area could be optimally increased by long gill filaments with large lamellae and this has subsequently been documented in numerous groups of fishes, including some African swamp teleosts living in hypoxic waters (Chapman, 2007) and some marine species living within the oxygen minimum layer (OML) (Graham, 2006).

While the gill morphometrics recruited to increase gill surface area appear consistent in a number of species, other fishes are unlikely to con-

---

Contract grant sponsor: National Science Foundation; Contract grant number: IOS-0817774; Contract grant sponsors: Tuna Industry Endowment Fund at Scripps Institution of Oceanography, William H. and Mattie Wattis Harris Foundation, Pfleger Institute of Environmental Research, George T. Pfleger Foundation, Moore Family Foundation, Nadine A. and Edward M. Carson Scholarship in conjunction with Achievement Rewards for College Scientists (ARCS), Los Angeles Chapter, the Edna Bailey Sussman Foundation.

\*Correspondence to: Nicholas C. Wegner, Scripps Institution of Oceanography, UCSD, 9500 Gilman Dr. Mailcode: 0204, La Jolla, CA 92093-0204. E-mail: nwegner@ucsd.edu

Received 12 March 2009; Revised 25 May 2009; Accepted 31 May 2009

Published online 5 August 2009 in Wiley InterScience (www.interscience.wiley.com)  
DOI: 10.1002/jmor.10777

form to these “rules of assembly.” Specifically, fast, continuously swimming teleosts such as scombrids (tunas, bonitos, and mackerels) and billfishes (marlins and swordfish) differ from other teleosts by having metabolic demands that are greater than those of other fishes (Brill, 1979, 1987; Brill and Bushnell, 1991; Dewar and Graham, 1994; Korsmeyer and Dewar, 2001), and by utilizing ram ventilation, the mechanism in which the forward momentum of continuous swimming is the driving force for ventilatory water flow through the gills (Roberts, 1975; Freadman, 1981; Roberts and Rowell, 1988). While tuna gill morphometrics have been studied (Muir and Hughes, 1969), a more comprehensive sampling of pelagic teleosts, ranging in aerobic capacity, is needed for insight into the selective effects of metabolic demand and ram ventilation on gill area and dimensions.

Tunas (family Scombridae) differ from other pelagic teleosts including other scombrids (mackerels, Spanish mackerels, wahoo, bonitos) in having a unique anterior and central positioning of the red (aerobic) swimming musculature coupled with counter-current heat exchangers (*retia mirabilia*) that allows for the retention of body heat produced through continuous swimming and ultimately increases muscle-power output and other metabolic functions (Carey and Teal, 1966; Altringham and Block, 1997; Graham and Dickson, 2001). The conservation of metabolically produced heat in the red muscle, eye and brain, and in some species, the viscera, its concomitant effects on the different tissues, and the high somatic and gonadal growth rates of tunas, all increase their metabolic demands above that of other fishes (Korsmeyer and Dewar, 2001). Oxygen acquisition in tunas is augmented through disproportionately large gill surface areas, which are as much as an order of magnitude larger than those of other marine teleosts (Muir and Hughes, 1969; Palzenberger and Pohla, 1992). Additional tuna gill specializations include thin diffusion distances and an unconventional diagonal blood-flow pattern through the lamellae that appears to optimize gas transfer (Muir, 1970; Muir and Brown, 1971; Olson et al., 2003; Wegner et al., 2006). A series of unique fusions connecting the gill filaments and lamellae function to support tuna gills against the forces of ram ventilation (Muir and Kendall, 1968; Johnson, 1986; Wegner et al., 2006).

Within the Scombridae, the sequence of evolutionary changes (from mackerel, less derived, to tunas, most derived) has been well documented in terms of gross muscle and skeletal morphology (Graham and Dickson, 2000; Collette et al., 2001) locomotor adaptations (Magnuson, 1978; Westneat and Wainwright, 2001), swimming biomechanics (Donley and Dickson, 2000; Altringham and Shadwick, 2001; Dowis et al., 2003), thermoregulation

(Graham and Dickson, 2000, 2001), and energetics (Sepulveda and Dickson, 2000; Korsmeyer and Dewar, 2001; Sepulveda et al., 2003). However, the evolutionary progression of changes in gill morphology remains generally unstudied. Limited gill surface area measurements for some non-tuna scombrids have been published (Gray, 1954; Steen and Berg, 1966; Hughes, 1970, 1972), but the small sample size and limited body-size range of the specimens examined preclude accurate interspecies comparison. With the exception of gill area estimates for the dolphinfish, *Coryphaena hippurus* (Hughes, 1970), even less is known for non-scombrid, high-energy demand teleosts. As a result, there has been little consideration of how groups such as the billfishes (families Xiphiidae, Istiophoridae) relate to tunas in terms of gill morphology. Although billfishes lack the red-muscle endothermy of tunas, they possess a number of features related to fast and continuous swimming (Dobson et al., 1986; Davie, 1990; Dickson, 1995), including gill-supporting fusions that appear to rival tunas in structural complexity (Johnson, 1986; Wegner et al., 2006).

This study examines the gill morphometry of five active pelagic teleosts (three non-tuna scombrids and two billfish species) for comparison with tunas, and investigates the rules of assembly governing the optimization of gill design in these fishes to meet requirements for high rates of gas transfer and ram ventilation.

## MATERIALS AND METHODS

Total gill surface areas were determined for three non-tuna scombrid species: Eastern Pacific bonito, *Sarda chiliensis* ( $n = 8$ , 0.2–6.4 kg), wahoo, *Acanthocybium solandri* ( $n = 8$ , 2.1–24.2 kg), and Pacific chub mackerel, *Scomber japonicus* ( $n = 8$ , 95–740 g), and two species of billfish: Striped marlin, *Kajikia audax* ( $n = 7$ , 8.0–70.0 kg), and swordfish, *Xiphias gladius* ( $n = 4$ , 22.0–125.1 kg). Gill areas were also determined for one skipjack tuna, *Katsuwonus pelamis* (3.4 kg), and one yellowfin tuna, *Thunnus albacares* (4.3 kg) to verify that the analytical methods used in this study yielded results that were consistent with previous work (Muir and Hughes, 1969).

## Gill Collection

Specimens were collected by hook and line off the coasts of Southern California and Hawaii, USA and Baja California, Mexico. Fish were euthanized immediately upon capture by surgically severing the spinal cord in accordance with Protocol S00080 of the University of California, San Diego Institutional Animal Care and Use Committee. Fish mass was determined by electronic scale or, when direct measurement was not possible, by using weight-length regression equations for the different species (Chatwin, 1959; Ponce-Diaz et al., 1991; DeMartini et al., 2000; Beerkircher, 2005).

Freshly euthanized specimens were placed ventral side up in a V-shaped cradle and the gills were irrigated with aerated sea water. The gills received one of two treatments. 1) Gills from approximately one half of the specimens were immediately excised and placed in 10% formalin buffered in seawater. 2) Gills from the remaining specimens were perfused with vascu-

lar casting solution (Mercox, Ladd Research, Williston, VT) according to methods described in Wegner et al. (2006). For this treatment, the heart was exposed by midline incision, cannulated, and specimens were perfused with heparinized teleost saline (Brill and Dizon, 1979) followed by the casting solution. Perfusions were conducted at physiological pressures (70–100 mmHg) consistent with those used in a previous study of tuna gill casting (Olson et al., 2003) to prevent rupturing and possible over-inflation of the gill blood vessels. Following perfusion, irrigation of the gills with sea water continued until complete polymerization of the casting solution (<15 min following injection), at which point the four gill arches from one side of each fish were placed into 10% formalin buffered in seawater. The other four arches were macerated in 15–20% KOH to remove all of the tissue from the casts.

### Total Gill Surface Area

Gill surface areas were estimated using methods established by Muir and Hughes (1969) and (Hughes, 1984b), and calculated by the equation:

$$A = L_{\text{fil}} \times 2n_{\text{lam}} \times A_{\text{lam}}$$

where  $A$  is total gill surface area,  $L_{\text{fil}}$  is the total length of all of the gill filaments,  $n_{\text{lam}}$  is lamellar frequency [the mean number of lamellae per unit length on one side of a filament (this is multiplied by two to account for the lamellae on both sides of each filament)], and  $A_{\text{lam}}$  is the mean bilateral surface area of a lamella.

For each specimen, all of the filaments on the four gill arches from one side of the head were counted. In specimens having more than 300 filaments per gill hemibranch, the filaments were divided into bins of 40 and the length of the medial filament (i.e., 20, 60, 100th, etc.) was determined and assumed to represent the average filament length for that bin. For individuals with fewer than 300 filaments per hemibranch, a bin size of 20 was used. Filament lengths were measured using fixed (or cast and subsequently fixed) material. Macerated vascular casts were not used to make this measurement because the casting solution did not always penetrate to the tip of each filament and would thus cause underestimation of length. Total filament length was calculated by combining the length determinations for each bin on each arch from one side of the head and then doubling this quantity to account for the filaments of the four gill arches on the other side of the head that were not measured.

Preliminary morphometric comparisons for all gill arches revealed that filaments on the third arch were most representative of average lamellar frequency and bilateral surface area, and further examination revealed that the anterior and posterior hemibranchs of gill arch three did not differ significantly with respect to these dimensions. Accordingly, all lamellar frequency and bilateral surface area data were obtained from the anterior hemibranch of the third gill arch. The medial filament of each bin from this hemibranch was removed from the arch, rinsed in deionized water, dehydrated in ethanol (20–25% increments over 24 hours), and critical-point dried to facilitate the acquisition of digital images and the removal of intact lamellae from the base, middle, and tip of each filament. Digital images were acquired using a camera mounted on a light microscope and analyzed using NIH Image J computer software to determine lamellar frequencies and areas. Vascular-cast filaments from the third gill arch were also sampled, photographed using a light microscope, and analyzed. Comparison of cast and critical-point-dried lamellae revealed that some shrinkage of lamellar bilateral surface area occurred during the drying process. For specimens not perfused with vascular casting solution, lamellar areas were thus adjusted by a species-specific correction factor that was determined by comparing cast and noncast lamellae.

### Lamellar Blood Flow

Cast gill material was also examined for comparison with previous studies which have described a unique diagonal pattern of blood flow through the lamellae of some scombrids and billfishes (Muir, 1970; Muir and Brown, 1971; Olson et al., 2003; Wegner et al., 2006). Twenty cast lamellae from each specimen were randomly sampled and viewed under low-vacuum mode using an FEI Quanta 600 scanning electron microscope. Acquired digital images of the lamellae were analyzed using Image J; the angle of blood flow relative to the lamellar long axis was measured midway along the length of each lamella.

### Statistical Analysis

For each species, total gill surface area ( $A$ ) and corresponding gill dimensions ( $L_{\text{fil}}$ ,  $n_{\text{lam}}$ ,  $A_{\text{lam}}$ ) were plotted in relation to body mass and linear regression equations were calculated. Regression lines for the different species were compared using 10,000 bootstrap replications (R v2.7.0) of the raw data, and statistical difference between species was determined if less than 5% of the resultant regression replicas intersected within the overlapping body-mass range of the species being compared. Species that did not overlap in mass were not compared statistically. The scaling exponents of the regressions were also compared to predictions assuming isometric scaling of gill growth using 95% confidence intervals. Finally, the angles of lamellar blood flow were compared between species using a one-way ANOVA in conjunction with a Tukey test.

## RESULTS

### Gill Surface Area

Figure 1 shows the total gill surface area in relation to body mass for the species examined in this study together with data for tunas (Muir and Hughes, 1969) and other marine teleosts (Hughes, 1970; Palzenberger and Pohla, 1992). Estimates of total gill surface area for the 3.4 kg skipjack tuna and 4.2 kg yellowfin tuna made in this study fit on the regressions determined for the same species by Muir and Hughes (1969) (Note: Muir and Hughes reported bluefin tuna, *Thunnus thynnus*, and yellowfin tuna data together as a single bluefin-yellowfin tuna regression). The consistency of data between the two reports confirms the morphometric methods used in this study and verifies that the skipjack tuna has the largest relative gill surface area of any teleost species examined to date. When compared over their shared ranges of body mass, skipjack tuna have significantly larger gill surface areas than those of bluefin-yellowfin tuna, eastern Pacific bonito, and wahoo. Bluefin-yellowfin tuna have significantly larger gill areas than those of bonito, wahoo, swordfish (when fish mass is greater than 29.93 kg), and striped marlin. Bonito gill areas are significantly larger than those of wahoo throughout the majority of their overlapping weight range ( $P < 0.05$  when fish mass is greater than 2.72 kg), but are not significantly greater than those of Pacific chub mackerel. Wahoo gill areas do not differ significantly from those of striped marlin and appear less than those



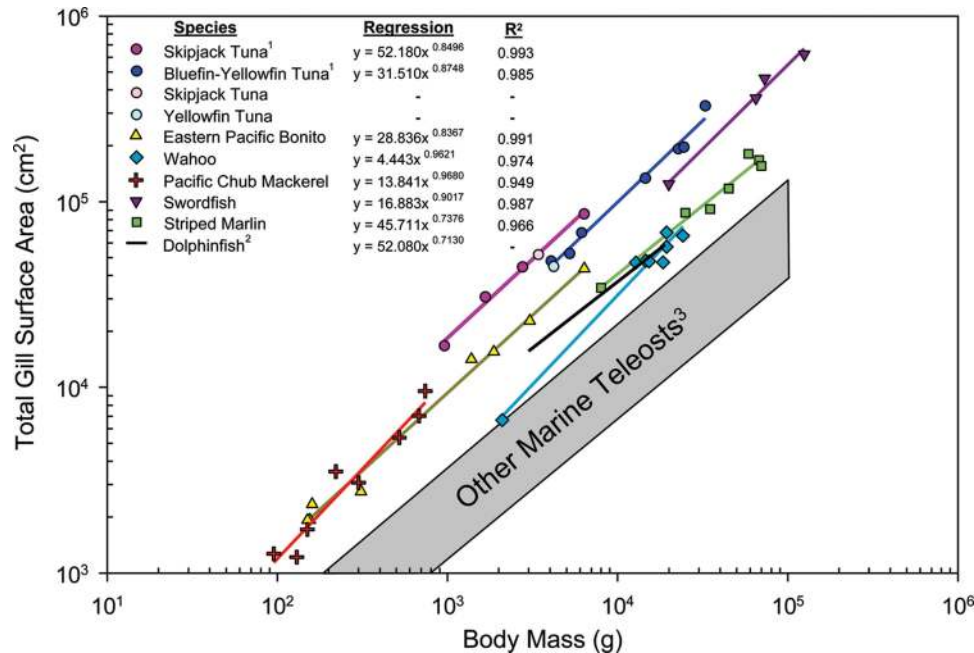


Fig. 1. Linear regressions showing the relationship of total gill surface area ( $\text{cm}^2$ ) and body mass (g) for the scombrids and billfishes examined in this study. Also included for comparison are gill area regressions for three species of tuna, dolphinfish, and a range of values compiled for other marine teleosts. Sources: <sup>1</sup>Muir and Hughes (1969). <sup>2</sup>Hughes (1970). <sup>3</sup>Palzenberger and Polha (1992). [Color figure can be viewed in the online issue, which is available at [www.interscience.wiley.com](http://www.interscience.wiley.com).]

of swordfish (however, the later relationship is not significant due to the small swordfish sample size). Swordfish have larger gill areas than those of striped marlin for the majority of their overlapping weight range ( $P < 0.05$  when fish mass is greater than 34.78 kg).

The scaling exponents of gill surface area to body mass for the species examined range from 0.74 to 0.97, which is within the range found in other teleosts (Hughes, 1972; De Jager and Dekkers, 1975; Palzenberger and Pohla, 1992). These scaling exponents are higher than that predicted by geometric similarity assuming isometric gill growth (0.67); the 95% confidence intervals for bluefin-yellowfin tuna (0.7576–1.0070), bonito (0.7549–0.9185), wahoo (0.8066–1.1176), and mackerel (0.7440–1.1920) all fall above this prediction.

### Total Filament Length

Regressions for total filament length and body mass are shown in Figure 2. Skipjack tuna total filament length is not larger than that of bluefin-yellowfin tuna, but is significantly greater than that of both bonito and wahoo. Bluefin-yellowfin tuna total filament length is also significantly larger than that of bonito and wahoo, but does not differ statistically from that of striped marlin. Bonito total filament length does not differ signifi-

cantly from that of wahoo or mackerel for most of their overlapping range of body mass.

Total filament length in swordfish appears greater than in bluefin-yellowfin tuna, wahoo, and striped marlin (Fig. 2); however, because of the limited swordfish sample size, total filament length is only significantly different with respect to striped marlin ( $P < 0.05$  when fish mass is greater than 42.19 kg). The high total filament length of swordfish results from a unique branching of the gill filaments (Fig. 3). Although filament branching in the swordfish occurs throughout each gill hemibranch, it is most elaborate on filaments originating near the acute angle formed by the ceratobranchial-epibranchial joint of the gill arch (Fig. 3A,C). The small number of filaments emanating from the gill arch at this location branch extensively to fill the area created as the filaments radiate outward. The widespread filament branching observed in swordfish was not present in the other pelagic teleosts examined (e.g., Fig. 3B,D for striped marlin). Although a few isolated cases of filament branching were observed in striped marlin, these often appear to be associated with filament regeneration following gill damage and are not inherent structural features of the gill that increase surface area.

The scaling exponents for total filament length in the scombrids and billfishes examined extend from 0.26 to 0.48, which range is similar to that

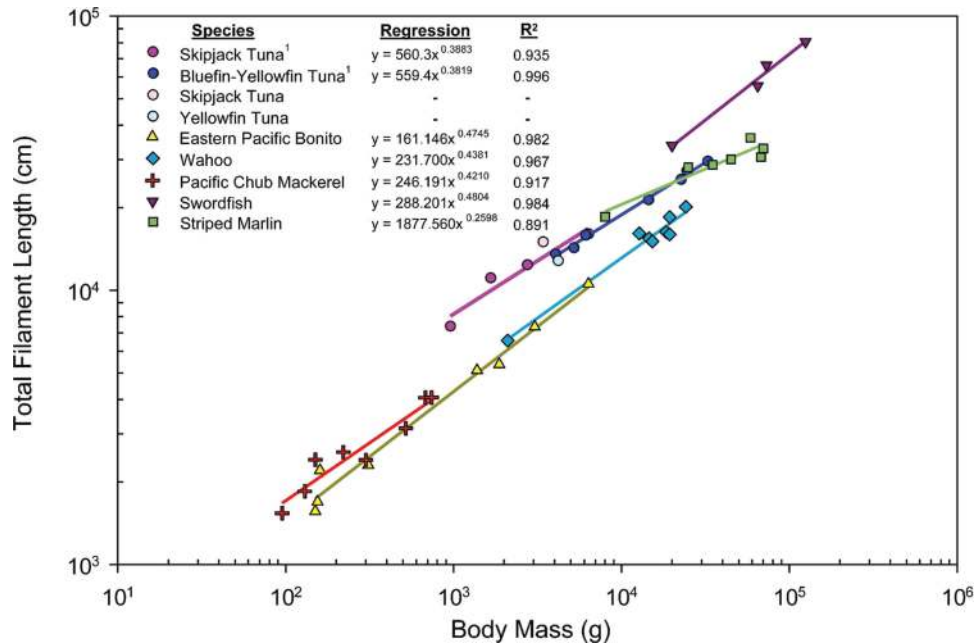


Fig. 2. Linear regressions relating total gill filament length (cm) to body mass (g) for the high-energy demand teleosts examined in this study together with data for three species of tuna from <sup>1</sup>Muir and Hughes (1969). [Color figure can be viewed in the online issue, which is available at [www.interscience.wiley.com](http://www.interscience.wiley.com).]

found in other teleosts (0.28–0.52) (Hughes, 1972; Palzenberger and Pohla, 1992).

It is important to further note that the gill dimension “total filament length” has two constituent parts: the average length of the gill filaments (average filament length) and their total number (total filament number). For each species, regressions for the two components were determined in relation to body mass, and these are shown in Table 1. Wahoo average filament length is significantly less than that of skipjack tuna, bluefin-yellowfin tuna, bonito, and striped marlin. Other interspecies comparisons do not show any significant differences. For total filament number, bonito have significantly fewer filaments than skipjack tuna, bluefin-yellowfin tuna, and wahoo. Examination of the regression lines shows that like bonito, mackerel also possess fewer filaments than the other pelagic teleosts examined; however, because the body-mass range of mackerel does not overlap with that of the other teleosts, this difference was not quantified statistically. Swordfish were not included in these analyses because the unique branching of the gill filaments prevents accurate comparison with other species.

### Lamellar Frequency

Regressions in Figure 4 compare the number of lamellae per mm of filament as a function of body mass. Skipjack tuna lamellar frequency per mm is not significantly different from that of bluefin-

yellowfin tuna or bonito, but is greater than that of wahoo ( $P < 0.05$  when fish mass is less than 6.22 kg). The lamellar frequency in bluefin-yellowfin tuna is significantly greater than in swordfish and striped marlin ( $P < 0.05$  for most of their shared weight range), but lower than in bonito. In addition to bluefin-yellowfin tuna, the lamellar frequency of bonito also is significantly greater than that of wahoo and striped marlin, but is significantly less than that of mackerel. Wahoo lamellar frequency is greater than that of swordfish and striped marlin ( $P < 0.05$  for most of their overlapping body-mass range). Swordfish have a significantly lower lamellar frequency than that of striped marlin.

The scaling exponents for lamellar frequency and body mass for the pelagic teleosts examined range from  $-0.089$  to  $0.006$ , which falls within the range determined for other bony fishes (Hughes, 1972; Palzenberger and Pohla, 1992).

### Lamellar Area

Regressions for lamellar bilateral surface area in relation to body mass are shown in Figure 5. The average lamellar surface area of skipjack tuna is significantly larger than that of bluefin-yellowfin tuna and wahoo ( $P < 0.05$  for most of the overlapping range of body mass), but does not differ significantly from that of bonito. Bluefin-yellowfin tuna lamellar area is significantly larger than that of wahoo and striped marlin, but is not statisti-

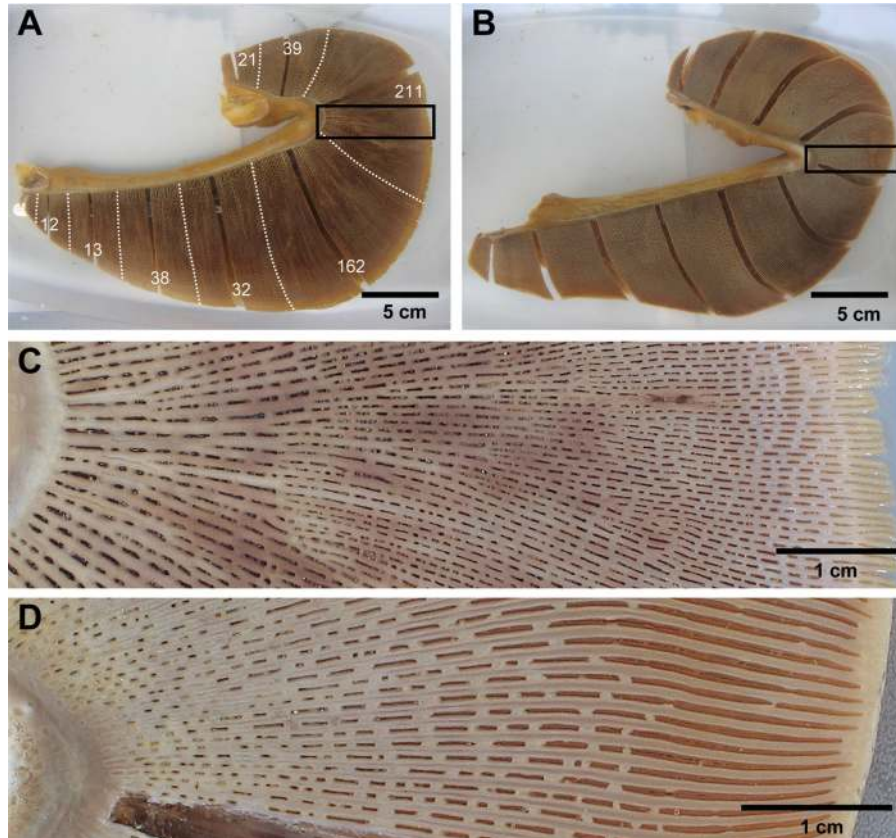


Fig. 3. Comparison of the anterior hemibranch of the third gill arch in (A) a 64.9 kg swordfish and (B) a 67.8 kg striped marlin. Dotted white lines on the swordfish gill arch distinguish bins of 40 filaments, and the number of branching events in each bin is listed. The medial filaments of each bin (dark areas) were removed for gill area measurements on the lamellae (i.e., determination of lamellar frequency and bilateral surface area). (C) Enlarged view of the box in A showing the details of swordfish filament branching. (D) Enlarged image of box in B detailing the nonbranching filaments of striped marlin. [Color figure can be viewed in the online issue, which is available at [www.interscience.wiley.com](http://www.interscience.wiley.com).]

cally different from that of bonito or swordfish. Bonito lamellar area is greater than that of wahoo for most of their shared weight range, but does not differ significantly from that of mackerel. The average bilateral lamellar area of wahoo does not differ significantly from that of striped marlin and is significantly less than that of swordfish.

Swordfish lamellar area is significantly greater than that of striped marlin.

The scaling exponents of lamellar area and body mass range from 0.41 to 0.58 for the pelagic teleosts examined and fall within the range reported for other teleosts (Hughes, 1972; Palzenberger and Pohla, 1992).

TABLE 1. Regression equations for average filament length and total filament number in relation to body mass for the species examined

Species	Average filament length		Total filament number	
	Regression	$R^2$	Regression	$R^2$
Skipjack Tuna	$y = 0.2221x^{0.2804}$	0.945	$y = 2532.30x^{0.1075}$	0.904
Bluefin-Yellowfin Tuna	$y = 0.1366x^{0.3360}$	0.977	$y = 4097.51x^{0.0458}$	0.406
Eastern Pacific Bonito	$y = 0.1193x^{0.3476}$	0.979	$y = 1341.02x^{0.1277}$	0.926
Wahoo	$y = 0.0734x^{0.3667}$	0.973	$y = 3156.89x^{0.0714}$	0.463
Pacific Chub Mackerel	$y = 0.1208x^{0.3453}$	0.936	$y = 2036.75x^{0.0758}$	0.656
Striped Marlin	$y = 0.2304x^{0.2824}$	0.956	$y = 6295.58x^{0.0040}$	0.005

Regressions for skipjack tuna and bluefin-yellowfin tuna were calculated using data from Muir and Hughes (1969).

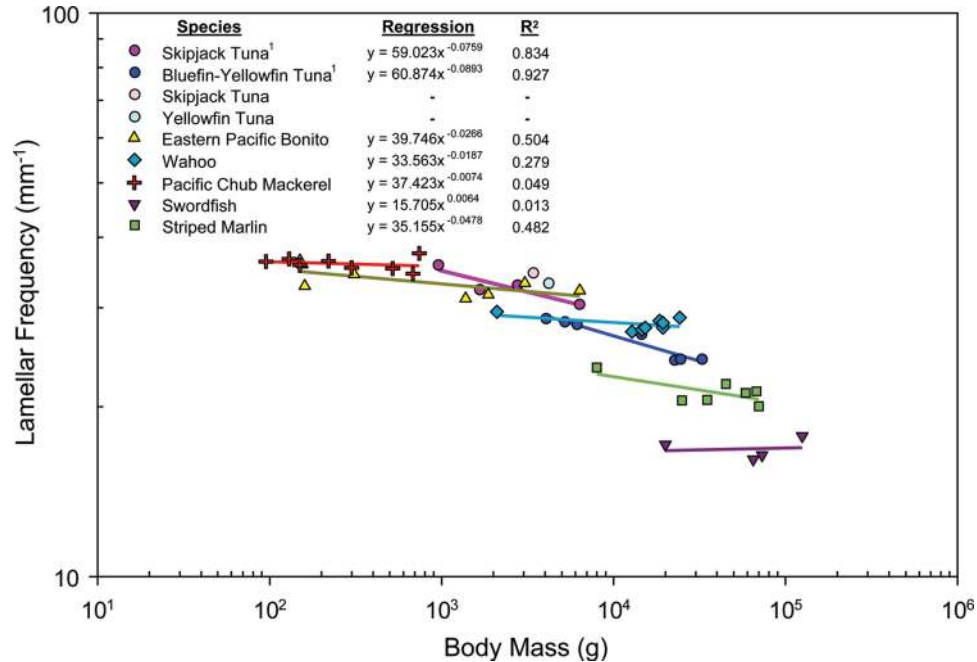


Fig. 4. Linear regression functions for lamellar frequency (average number of lamellae per millimeter on one side of a gill filament) and body mass (g) for the pelagic teleosts examined. Also shown are data for three species of tuna from <sup>1</sup>Muir and Hughes (1969). [Color figure can be viewed in the online issue, which is available at [www.interscience.wiley.com](http://www.interscience.wiley.com).]

### Lamellar Shape and Blood Flow

The lamellae of the examined pelagic teleosts are rectangular and have a high aspect ratio (i.e., they are several times longer than they are high). This

differs from the lamellae of most other teleosts, which have a lower aspect ratio and are frequently triangular or semicircular (Hughes, 1970; Hughes and Morgan, 1973). Associated with the high aspect

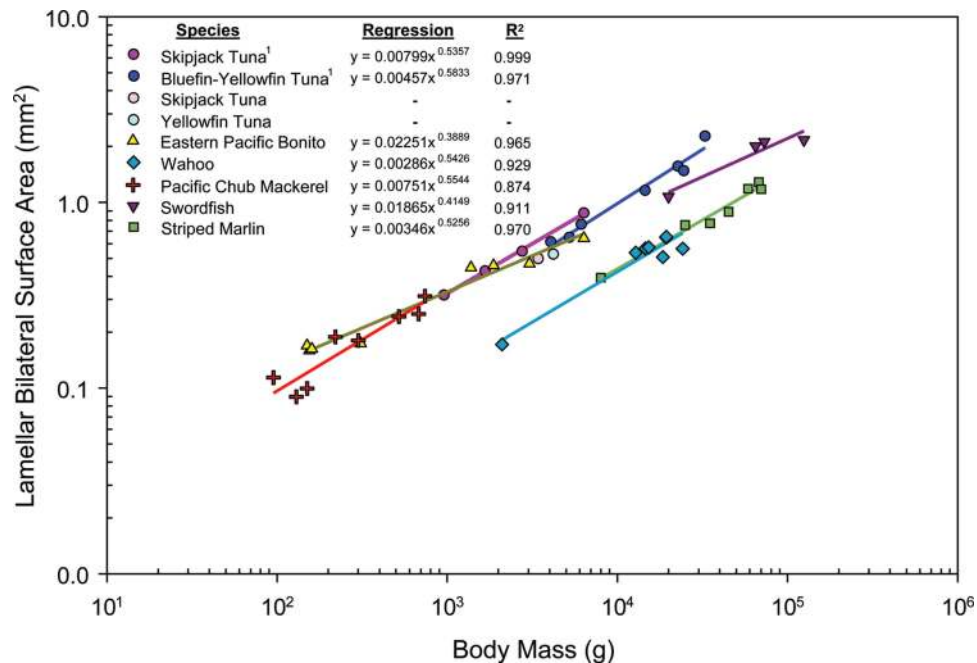


Fig. 5. Linear regressions for lamellar bilateral surface area (mm<sup>2</sup>) and body mass (g) for the scombrids and billfishes in this study. Data for three species of tuna are from <sup>1</sup>Muir and Hughes (1969). [Color figure can be viewed in the online issue, which is available at [www.interscience.wiley.com](http://www.interscience.wiley.com).]



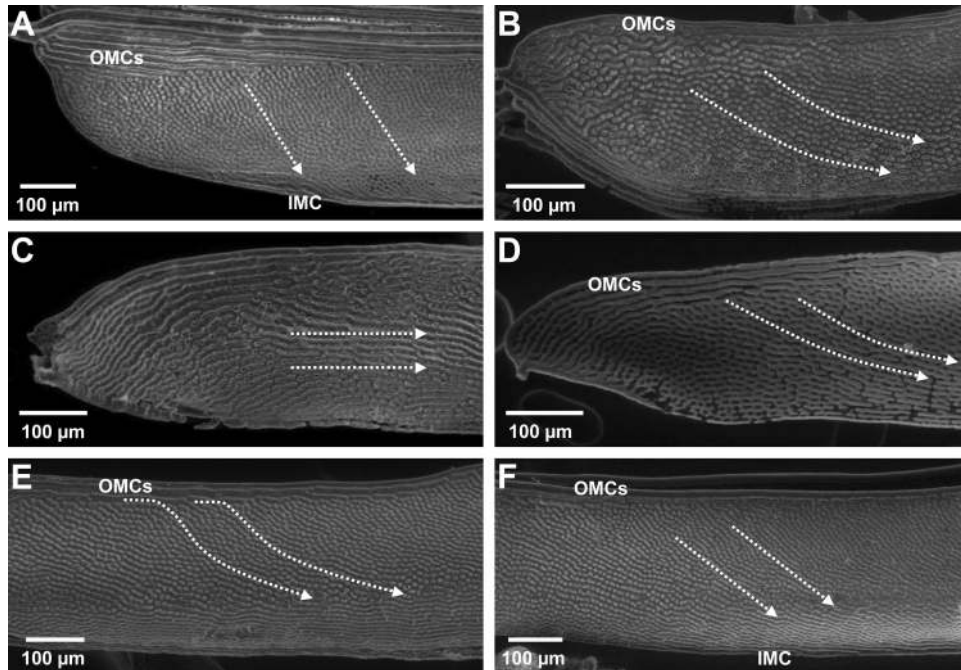


Fig. 6. Microvascular-cast gill lamellae from (A) a 4.2 kg yellowfin tuna, (B) a 1.87 kg eastern Pacific bonito, (C) a 15.3 kg wahoo, (D) a 0.74 kg Pacific chub mackerel, (E) a 20.0 kg swordfish, and (F) a 45.0 kg striped marlin. Dotted arrows indicate the pathway of blood flow. Water flow is from right to left in all images. Abbreviations: IMC, inner marginal channel; OMC, outer marginal channel.

ratio of scombrid and billfish lamellae are lamellar blood-flow patterns that usually differ from those of other fishes; these are shown in Figure 6 and some of the related features are quantified in Table 2. The pattern of lamellar blood flow observed for the tunas in this study is consistent with previous reports (Muir, 1970; Muir and Brown, 1971; Olson et al., 2003; Wegner et al., 2006), and the yellowfin tuna blood-flow pattern is shown in Figure 6A. Blood entering tuna lamellae proceeds into a series of outer marginal channels (OMCs) extending along the lamellar lateral edge and is then directed (by

the unique placement of lamellar pillar cells) diagonally across the lamellae at an angle of 50–60° relative to the lamellar long axis; efferent blood is collected by an inner marginal channel (IMC). In the eastern Pacific bonito (Fig. 6B), the angle of diagonal flow with respect to the lamellar axis is reduced in comparison to that of tunas. Also, the diagonal flow does not extend across the entire lamellar height, and therefore, blood is not collected by a single IMC. Wahoo lamellar blood flow does not show a diagonal progression, but rather advances parallel to the lamellar long axis (Fig. 6C) and is

TABLE 2. Angle of lamellar blood flow (measured relative to the lamellar long axis) and related features (distribution of blood to the lamellae by outer marginal channels, collection of blood in an inner marginal channel) in the pelagic teleosts examined

Species	n	Weight range (kg)	Mean blood-flow angle $\pm$ SD	OMCs	IMC
Skipjack Tuna	1	3.4	61.5 $\pm$ 6.3	Yes	Yes
Yellowfin Tuna	1	4.3	48.5 $\pm$ 10.3	Yes	Yes*
Eastern Pacific Bonito	4	0.2–1.9	31.9 $\pm$ 6.7	Yes	No
Wahoo	3	12.8–19.4	0	No	No
Pacific Chub Mackerel	5	0.1–0.7	20.1 $\pm$ 7.2	Yes	No
Swordfish	3	20.0–125.1	29.9 $\pm$ 6.3	Yes	No
Striped Marlin	3	8.0–56.8	36.3 $\pm$ 6.7	Yes	Yes

All interspecies comparisons of blood-flow angle are significantly different with the exception of eastern Pacific bonito and swordfish. Abbreviations: IMC, inner marginal channel; OMC, outer marginal channel; SD, standard deviation.

\*In some of the small yellowfin tuna lamellae sampled, diagonal blood flow did not extend across the entire lamellar height and therefore was not collected by an inner marginal channel.



thus similar to that of most fishes. The Pacific chub mackerel lamellar blood-flow pattern (Fig. 6D) is similar to that of bonito; however, the angle of diagonal flow is further reduced from that of tunas ( $\sim 20^\circ$ ) and is less than that reported by Muir and Brown (1971) for a single specimen of Atlantic chub mackerel, *Scomber scombrus* ( $\sim 35^\circ$ ). The swordfish lamellar blood-flow pattern (Fig. 6E) is also similar to that of bonito. Although the angle is less than that of skipjack tuna and yellowfin tuna (Table 2), striped marlin lamellar blood flow is similar to that of tunas in that diagonal flow extends across the entire lamellar height and is collected in an IMC (Fig. 6F).

## DISCUSSION

This study confirms the large gill surface areas of tunas and shows that the gill areas of non-tuna scombrids and billfishes, while not as high as those of tunas, are larger than those of most other fish species. The morphometric parameters underlying the large gill surface areas of tunas include: 1) a high total filament length resulting from a large number of long gill filaments, 2) a high lamellar frequency, and 3) lamellae that, although not larger in area than those of other species, have a high-aspect ratio (i.e., they are long but not high) and are thus optimally shaped for the close-proximity packing of gill filaments. The non-tuna scombrids and billfishes examined utilize these same features to increase gill surface area, however, to a lesser extent than tunas. This section compares the gill morphometry of the scombrid and billfish species studied and examines the influence of both ram ventilation and metabolic demand in the sculpting of gill dimensions.

### Scombrids

The species examined in this study represent four scombrid tribes (Scombrini = mackerels, Scomberomorini = Spanish mackerels and wahoo, Sardini = bonitos, and Thunnini = tunas), and Figure 7 shows their phylogenetic relationship. Previous research comparing these tribes has readily demonstrated the sequential increase in adaptations for high-performance swimming from mackerels to tunas (Magnuson, 1978; Collette et al., 2001; Graham and Dickson, 2001; Korsmeyer and Dewar, 2001). However, while tunas have larger gill surface areas than other scombrids, there is not a progressive increase in this feature within the clade; the gill areas of mackerel and bonito are similar, and the wahoo has a relatively smaller gill surface area than that of the mackerel (Fig. 1), despite its closer relationship to tunas (Fig. 7). Likewise, there are not emergent patterns for graded changes in the gill-area dimensions among the genera examined. For example, bonito and mackerel show little difference in their gill morphometrics (Figs. 2, 4, and 5).

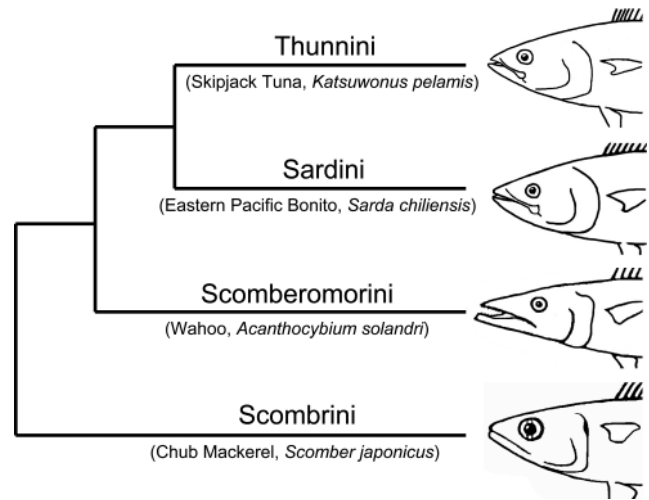


Fig. 7. Scombrid phylogeny showing the four tribes of the subfamily Scombrinae and a species from each tribe examined in this study.

Tuna gill surface area is augmented above that of their scombrid relatives by a higher total filament length (Fig. 2). This results from relatively more gill filaments than in both bonito and mackerel, and longer gill filaments than in wahoo (Table 1). Figure 8 shows how the lamellar shape of tunas decreases interfilament spacing and allows for a high filament number. In addition, because tunas are obligate ram ventilators, and thus do not use the opercular chambers to induce branchial flow, this may allow them to more fully utilize this space to increase filament length. Although less than that of tunas, the other scombrid species examined also have a relatively higher total filament length than that of most other teleosts. Bonito and mackerel gill filaments are as long as those of tunas, but are not as numerous (Table 1). In contrast, the long and slender head of the wahoo (Fig. 7) allows for a high filament number, but limits filament length (Table 1).

A common feature in the gills of all scombrids is a high lamellar frequency. Concomitant with this is a short interlamellar spacing (which minimizes physiological dead space) and a reduction in the thickness of the lamellae. Scombrid lamellar thickness is only about 5–6  $\mu\text{m}$  (Wegner et al., 2006) and is associated with a thin respiratory epithelium (water-blood barrier distance) of only 0.5–1.2  $\mu\text{m}$  (Hughes, 1970; Wegner et al., 2006), which can be more than an order of magnitude less than that of other fishes (range 2–11  $\mu\text{m}$ ) (Piiper, 1971; Hughes and Morgan, 1973). Thus, in addition to allowing for a high lamellar frequency, the close spacing and reduction in lamellar thickness also decrease diffusion distances for gas exchange.

The lamellae of scombrids are also long and low in profile, and this is associated with an atypical diagonal blood-flow pattern through the lamellae

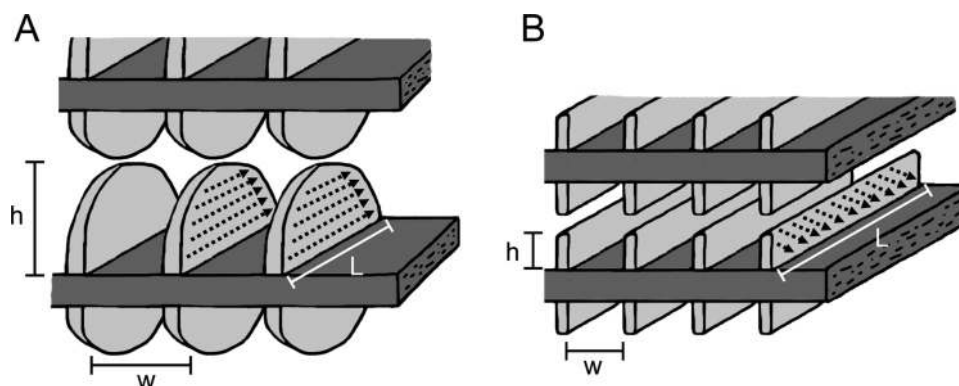


Fig. 8. Generalized comparison of the gill filaments (dark gray) and lamellae (light gray) for (A) most teleosts and (B) most scombrids and billfishes. Lamellar blood-flow direction is indicated by dotted arrows; water flow between the lamellae is out of the page. Abbreviations: h, lamellar height; L, lamellar length; w, interlamellar channel width. Note: for simplicity, fusions of the gill filaments and lamellae are not shown for B.

of tunas, bonito, and mackerel. This diagonal pattern differs from that of other fishes, including the wahoo, in which blood flows parallel to and along the lamellar long axis (compare Fig. 6A,B, and D with 6C, and Fig. 8A with 8B) (Muir, 1970; Muir and Brown, 1971; Olson et al., 2003; Wegner et al., 2006). The diagonal pattern has been suggested as a mechanism that reduces the length of the lamellar blood pathway to that required for oxygen loading (i.e., blood channels running along the entire length of a lamella would be longer than necessary for complete gas exchange) (Muir, 1970; Muir and Brown, 1971; Olson et al., 2003; Wegner et al., 2006). Thus, the larger number of short, in-parallel blood vessels resulting from diagonal flow increases gas-exchange efficiency by more closely matching blood-resident and oxygen-loading times and permits the entire length of the lamella to function for gas exchange despite its long shape. In addition, because the diagonal blood channels are significantly shorter than lamellar length, this adaptation also reduces vascular resistance through the gills (Muir, 1970; Muir and Brown, 1971). The angles of diagonal blood flow in the lamellae of bonito ( $31.9 \pm 6.7^\circ$ ) and mackerel ( $20.1 \pm 7.2^\circ$ ) are much less than those of tunas ( $48.5 \pm 10.3^\circ$  for yellowfin and  $61.5 \pm 6.3^\circ$  for skipjack) (Fig. 6, Table 2). The decrease in the angle of diagonal flow results in a longer blood pathway through the lamellae, consequently increasing blood residence times, and likely indicates a reduced capacity for non-tuna scombrids to uptake oxygen in comparison to tunas.

### Billfishes

Swordfish and striped marlin are convergent with scombrids for the general features of gill design (i.e., high total filament lengths, a relatively high lamellar frequency, and long lamellae with diagonal blood flow) that augment gill surface

area. However, the extent to which the morphometrics are utilized differs slightly; both swordfish and striped marlin have lower lamellar frequencies than any of the scombrids examined (Fig. 4), which is compensated by relatively high total filament lengths (Fig. 2).

Swordfish gill surface area is markedly larger than that of striped marlin (Fig. 1). Morphometric comparisons reveal that although striped marlin lamellar frequency is significantly greater (Fig. 4), swordfish gill area is augmented by both a larger lamellar bilateral surface area (Fig. 5) and a higher total filament length (Fig. 2). The larger total filament length in the swordfish is derived from the unique branching of the gill filaments (Fig. 3). In addition to augmenting gill area, branching also appears to even the spacing between adjacent filaments. This is particularly apparent near the cerato-epibranchial joint where, with the acute intersection angle of the two bones, a relatively small number of filaments branch extensively to fill the expanding sector of the branchial cavity extending out from the gill arch (Fig. 3A,C). The resulting consistency in interfilament spacing likely encourages the uniform distribution of water flow between the filaments and to the lamellae. In contrast, the filaments leaving the cerato-epibranchial joint in the other pelagic teleosts examined (as seen for the striped marlin in Fig. 3B,D) are spaced close together near their origin, but separate as they radiate outward. Although this progressive increase in interfilament spacing away from the arch does not seem to result in morphological dead space [i.e., the lamellae appear to fully occupy this area (Fig. 3D)], water flow between the filaments may be less evenly distributed.

Although gill morphometric data are needed for other billfish species, the swordfish appears unique in having branching filaments and thus likely has

the largest relative gill surface area among all billfishes (blue marlin, *Makaira nigricans*, shortbill spearfish, *Tetrapturus angustirostris*, and round-scale spearfish, *Tetrapturus georgii*, all lack the extensive filament branching of the swordfish; Wegner, unpublished). The higher gill surface area of the swordfish may reflect differences from other billfishes in terms of metabolic demand, habitat utilization, or both. Although little is known about billfish metabolic requirements, swordfish differ greatly from other billfish species in terms of habitat exploitation. Tagging data show that swordfish spend most of the daylight hours at depth, often in excess of 400 m (Carey, 1990; Sepulveda et al., in review), while most other billfishes appear to be much more surface oriented (Block et al., 1992; Brill et al., 1993; Prince and Goodyear, 2006). In many regions, the depth at which swordfish spend significant time correlates with the OML where oxygen content can be below  $0.5 \text{ ml l}^{-1}$  (Conkright et al., 1998; Bograd et al., 2008). In contrast, both blue marlin and sailfish (*Istiophorus platypterus*) in the Eastern Tropical Pacific appear to be limited to the top 100 m of the water column where dissolved oxygen levels are greater than  $3.5 \text{ ml l}^{-1}$  (Prince and Goodyear, 2006). The large gill area of the swordfish may thus facilitate respiration in the OML and allow this species to exploit resources unavailable to other billfishes.

### Gill Morphometrics and Ram Ventilation

The gill dimensions contributing to the large gill surface areas of both scombrids and billfishes do not conform to predictions by Hughes (1966) that gill surface area is optimally increased by long gill filaments and large (tall) lamellae. Hughes based his predictions on the concept that gill morphometrics are a balance between optimizing gill surface area and minimizing gill resistance to water flow to conserve energy associated with actively pumping water through the gills. However, in scombrids and billfishes, the need to propel sufficient water over the gills, a fundamental paradigm of active ventilation, is reversed: these ram-ventilators have sufficient water flow; the need is to ensure the slow and uniform passage of water over the exchange surfaces and to maintain gill structural integrity in face of the high-pressure ventilatory stream.

While most scombrids and billfishes have relatively long gill filaments as predicted by Hughes (1966), total filament length is also increased in these fishes by numerous, tightly packed filaments. The close proximity of neighboring filaments necessarily requires a low lamellar height (Fig. 8), and the pelagic teleosts examined thus lack the large and tall lamellae predicted by Hughes (1966). In addition to allowing for extra gill filaments, the long rectangular shape of scombrid and billfish lamellae offers the following

advantages: 1) it allows for a longer axis for lamellar attachment to the gill filament, which likely increases lamellar rigidity opposing the forceful branchial flow associated with ram ventilation, 2) the low profile of the lamellae requires less structural support than tall lamellae, and thus the thickness of the lamellar epithelium can be reduced to decrease diffusion distances, 3) short diffusion distances allow lamellar blood to quickly load oxygen and thus vascular resistance can be minimized through short diagonal blood channels (discussed above), and 4) lamellar shape in conjunction with lamellar spacing increases gill resistance, which is likely necessary to slow and streamline branchial flow to create optimal conditions for gas exchange in the interlamellar spaces.

The lamellae are the primary site of gill resistance (Hughes, 1966; Brown and Muir, 1970), and according to Poiseuille's equations for water flow, this resistance is a function of both the length and width of the interlamellar channels (Fig. 8). To minimize resistance, and as predicted by Hughes (1966), many active-ventilating teleosts have relatively tall lamellae (which are not long) and wide interlamellar spaces. However, scombrids and billfishes have both narrow (due to high lamellar frequencies) and long interlamellar channels (Fig. 8) which increase gill resistance, and this appears to slow the ram ventilatory stream and optimize water residence times at the exchange surfaces. In swimming skipjack tuna, water entering the mouth is slowed by  $200\times$  to interlamellar velocities ranging from 0.13 to 0.75 cm/s (Brown and Muir, 1970; Stevens and Lightfoot, 1986), which speeds fall within the range reported for teleosts that rely upon active ventilation (Lauder, 1984).

In large scombrids (tunas of the genus, *Thunnus*, wahoo) and billfishes, water flow through the gills also encounters resistance in the form of filament fusions (shown in Fig. 3C for swordfish and 3D for striped marlin). These fusions are thought to provide added structural support to long gill filaments to counteract the tendency of the ram-ventilatory stream to deform the gills (Muir and Kendall, 1968; Johnson, 1986; Wegner et al., 2006). However, filament fusions may also function to help streamline water flow and encourage its uniform distribution to the gill lamellae. The fusions which, in most species line both the leading and trailing edges of the gill filaments, essentially encase the respiratory lamellae, and the resulting pores between juxtaposed fusions likely restrict both the speed and volume of water entering the lamellar channels (Muir and Kendall, 1968). This mechanism for streamlining branchial flow appears to lessen the need for a high lamellar frequency, and accordingly, a negative correlation is seen between lamellar frequency and the proliferation of filament fusions in the species examined; filament fusions are most extensive in swordfish (Fig. 3C), followed by striped marlin (Fig.



TABLE 3. Comparison of gill surface areas ( $\text{mm}^2 \text{g}^{-1}$ ) and standard metabolic rates (SMR,  $\text{mgO}_2 \text{kg}^{-1} \text{h}^{-1}$ ) for the high-energy demand teleosts in this study at a body mass of 1 kg (determined from gill area to body mass and SMR to body mass regressions)

Species	Gill area ( $\text{mm}^2 \text{g}^{-1}$ )	SMR ( $\text{mgO}_2 \text{kg}^{-1} \text{h}^{-1}$ )	SMR/gill area ( $\text{mgO}_2 \text{h}^{-1} \text{m}^{-2}$ )
Skipjack Tuna	1846 <sup>a</sup>	412 <sup>b</sup>	223.2
Yellowfin Tuna	1327 <sup>a</sup>	286 <sup>c</sup>	215.5
Eastern Pacific Bonito*	933 (1080) <sup>d</sup>	161 <sup>e</sup>	149.1
Wahoo	342 <sup>d</sup>	—	—
Pacific Chub Mackerel	1110 <sup>d</sup>	132 <sup>f</sup>	118.9
Swordfish	856 <sup>d</sup>	—	—
Striped Marlin	746 <sup>d</sup>	—	—

SMR data from the literature were determined for skipjack tuna at 23.5–25.5°C and for yellowfin tuna at 25°C. Bonito and mackerel SMRs were thus adjusted to 25°C using a  $Q_{10}$  of 2.

Sources:

<sup>a</sup>Muir and Hughes (1969).

<sup>b</sup>Brill (1979).

<sup>c</sup>Brill (1987).

<sup>d</sup>Present study.

<sup>e</sup>Sepulveda et al. (2003).

<sup>f</sup>Calculated from Sepulveda and Dickson (2000).

\*Sepulveda et al. (2003) made metabolic measurements on a limited size range of bonito and did not find a significant relationship between metabolic rate and body size; SMR data were thus pooled for all specimens (average body mass = 1191 g). For accurate determination of the SMR to gill area ratio, gill area was calculated for a fish of this size (shown in parentheses), and the SMR to gill area ratio reflects this body mass.

3D), and are less prevalent in wahoo and bluefin and yellowfin tunas. Correspondingly, lamellar density is lowest in swordfish (16–18  $\text{mm}^{-1}$ ), somewhat greater in striped marlin (20–24  $\text{mm}^{-1}$ ), and further increased in wahoo (27–29  $\text{mm}^{-1}$ ) and bluefin-yellowfin tuna (24–33  $\text{mm}^{-1}$ ). Lamellar frequency peaks (30–36  $\text{mm}^{-1}$ ) in skipjack tuna, bonito, and mackerel, which all lack filament fusions.

The selective pressures operating on the evolution of gill morphometrics in scombrids and billfishes thus appear to be a balance between the optimization of both gill resistance to provide favorable flow conditions through the lamellae and gill surface area to meet metabolic demands. However, unlike most teleosts in which resistance is thought to be minimized, scombrid and billfish evolution appears to have selected for higher gill resistance to streamline the high-speed ventilatory flow produced by ram ventilation, whether through high lamellar densities, filament fusions, or a combination of both. The negative correlation of lamellar frequency and the prevalence of filament fusions suggests that the high density of the gill lamellae may be more important in slowing and streamlining branchial flow induced by ram ventilation than it is in increasing gill surface area. This may explain why many marine teleosts which utilize ram ventilation while feeding or when swimming at faster speeds (e.g., menhaden, herring, bluefish, and some jack species) have high lamellar frequencies (Gray, 1954; Hughes, 1966; Piiper, 1971) despite metabolic demands that are assumedly less than those of scombrids and billfishes. Likewise, bonito and mackerel lamellar

frequencies are as high as or greater than those of tunas (Fig. 4), despite much smaller gill surface areas (Fig. 1).

### Gill Area and Metabolic Demand

While a high lamellar frequency appears linked to the use of ram ventilation, gill surface area as a whole tends to correlate with metabolic demand. Table 3 shows the relationship between gill area and standard metabolic rate (SMR) in the scombrids and billfishes for which data are available. The ratio of SMR to gill surface area appears fairly consistent (100–250  $\text{mgO}_2 \text{h}^{-1} \text{m}^{-2}$ ) within the species examined and argues for a direct correlation of gill surface area with metabolic requirements. The SMRs of Pacific chub mackerel and eastern Pacific bonito are similar (Sepulveda and Dickson, 2000; Sepulveda et al., 2003) and are matched by comparable gill areas. Tunas, having higher SMRs, possess correspondingly larger gill surface areas.

The general consistency of the ratio of SMR to gill area within the scombrids and billfishes examined provides insight into the metabolic requirements of large pelagic fishes for which SMR cannot be determined directly. Because of their size, pelagic habitat, and dependence on ram ventilation, many high-energy demand teleosts (i.e., certain tunas, the wahoo, and billfishes) cannot easily be caught at sea and returned to the laboratory for experimental determination of energetic requirements. Gill area measurements may thus serve as a proxy to estimate SMR which is an important

parameter in energetic, growth, and fisheries modeling. The similarity in the relative gill surface areas of billfishes and non-tuna scombrids suggests comparable aerobic demands for these two groups. However, the correlation between SMR and gill surface area may be altered by factors such as the exploitation of hypoxic habitats (De Jager and Dekkers, 1975; Mandic et al., 2009). The utilization of the OML by the swordfish may have been a key evolutionary driving force that led to its large gill surface area in comparison to other billfishes and does not necessarily indicate higher aerobic demands in swordfish than in its relatives. Additional insight into the effects of metabolic demand and habitat utilization on the gill dimensions of pelagic fishes would be gained by examining bigeye tuna, *Thunnus obesus*, which also frequents the OML and should have metabolic requirements similar to those of other tunas.

In addition to the effects of exploiting hypoxic habitats, the relationship of SMR and gill area can be compounded by scaling. In many teleosts, the scaling exponents of gill surface area to body mass and SMR to body mass are similar (average 0.75–0.85) (Hughes, 1984a; Palzenberger and Pohla, 1992), and this correlation has been suggested as the reason that the scaling exponent of gill surface area is often greater than that predicted by geometric similarity assuming isometric growth of the gills (scaling exponent = 0.67). However, the scaling exponents for SMR to body mass for skipjack tuna (0.50) (Brill, 1979) and yellowfin tuna (0.57–0.60) (Brill, 1987; Dewar and Graham, 1994) are significantly less than those of gill surface area to body mass (skipjack tuna = 0.85, bluefin-yellowfin tuna = 0.86). Consequently, the ratio of SMR to gill surface area varies as a function of body mass. Although these scaling effects may not change the general conclusions that can be drawn on how scombrid and billfish SMRs compare, the disparity in the scaling exponents of gill area and SMR in skipjack tuna and yellowfin tuna suggests other factors influence gill size. Hughes (1984a) and others have suggested that gill area may scale more consistently with routine or active metabolic rates, and for fish groups such as scombrids and billfishes this seems more appropriate as these fishes are continuous swimmers and never experience “rest” conditions.

## ACKNOWLEDGMENTS

The authors thank S. Aalbers, N. Ben-Aderet, D. Bernal, R. Brill, D. Cartamil, M. Domeier, T. Fullam, D. Fuller, M. Musyl, A. Nosal, N. Sepulveda, L. Williams, and the crews of the Polarix Supreme and Oscar Elton Sette who helped in specimen acquisition and vascular-casting perfusions, E. York of the SIO Analytical Facility for technical assistance with microscopy work, and C.

Anderson for help with statistical analyses. They also thank P. Hastings, M. McHenry, F. Powell, and R. Rosenblatt for reviewing versions of this manuscript.

## LITERATURE CITED

- Altringham JD, Block BA. 1997. Why do tuna maintain elevated slow muscle temperatures? Power output of muscle isolated from endothermic and ectothermic fish. *J Exp Biol* 200:2617–2627.
- Altringham JD, Shadwick RE. 2001. Swimming and muscle function. In: Block BA, Stevens ED, editors. *Tuna: Physiology, Ecology and Evolution*. San Diego: Academic Press. pp 313–344.
- Beerkircher LR. 2005. Length to weight conversions for wahoo, *Acanthocybium solandri*, in the Northwest Atlantic. *Col Vol Sci Papers ICCAT* 58:1616–1619.
- Block BA, Booth DT, Carey FG. 1992. Depth and temperature of the blue marlin, *Makaira nigricans*, observed by acoustic telemetry. *Mar Bio* 114:175–183.
- Bograd SJ, Castro CG, Di Lorenzo E, Palacios DM, Bailey H, Gilly W, Chavez FP. 2008. Oxygen declines and the shoaling of the hypoxic boundary in the California current. *Geophys Res Lett* 35:L12607.
- Brill RW. 1979. Effect of body size on the standard metabolic rate of skipjack tuna, *Katsuwonus pelamis*. *Fish Bull* 77:494–498.
- Brill RW. 1987. On the standard metabolic rates of tropical tunas, including the effect of body size and acute temperature change. *Fish Bull* 85:25–36.
- Brill RW, Bushnell PG. 1991. Metabolic and cardiac scope of high-energy demand teleosts, the tunas. *Can J Zool* 69:2002–2009.
- Brill RW, Dizon AE. 1979. Effect of temperature on isotonic twitch of white muscle and predicted maximum swimming speeds of skipjack tuna, *Katsuwonus pelamis*. *Env Biol Fish* 4:199–205.
- Brill RW, Holts DB, Chang RKC, Sullivan S, Dewar H, Carey FG. 1993. Vertical and horizontal movements of striped marlin (*Tetrapturus audax*) near the Hawaiian Islands, determined by ultrasonic telemetry, with simultaneous measurement of oceanic currents. *Mar Bio* 117:567–574.
- Brown CE, Muir BS. 1970. Analysis of ram ventilation of fish gills with application to skipjack tuna (*Katsuwonus pelamis*). *J Fish Res Bd Canada* 27:1637–1652.
- Carey FG. 1990. Further acoustic telemetry observations of swordfish. In: Stroud RH, editor. *Planning the Future of Billfishes*. Atlanta, Georgia: National Coalition for Maine Conservation. pp 103–122.
- Carey FG, Teal JM. 1966. Heat conservation in tuna fish muscle. *Proc Natl Acad Sci USA* 56:1461–1469.
- Chapman LJ. 2007. Morpho-physiological divergence across aquatic oxygen gradients in fishes. In: Fernandes MN, Rantin FT, Glass ML, Kapoor BG, editors. *Fish Respiration and Environment*. Enfield: Science Publishers. pp 13–39.
- Chatwin BM. 1959. The relationships between length and weight of yellowfin tuna (*Neothunnus macropterus*) and skipjack tuna (*Katsuwonus pelamis*) from the Eastern Tropical Pacific Ocean. *Inter-Amer Trop Tuna Comm Bull* 3:305–352.
- Collette BB, Reeb C, Block BA. 2001. Systematics of the tunas and mackerels (Scombridae). In: Block BA, Stevens ED, editors. *Tuna: Physiology, Ecology and Evolution*. San Diego: Academic Press. pp 5–30.
- Conkright M, Levitus S, O'Brien T, Boyer T, Antonov J. 1998. *World Ocean Atlas 1998*. CD-ROM Data Set Documentation. Silver Spring, MD: Technical Report 15, NODC Internal Report.
- Davie PS. 1990. *Pacific Marlins: Anatomy and Physiology*. Palmerston North, New Zealand: Simon Print. 88 p.
- De Jager S, Dekkers WJ. 1975. Relation between gill structure and activity in fish. *Neth J Zool* 25:276–308.

- DeMartini EE, Uchiyama JH, Williams HA. 2000. Sexual maturity, sex ratio, and size composition of swordfish. *Xiphias gladius*, caught by the Hawaii-based pelagic longline fishery. *Fish Bull* 98:489–506.
- Dewar H, Graham JB. 1994. Studies of tropical tuna swimming performance in a large water tunnel. 1. Energetics. *J Exp Biol* 192:13–31.
- Dickson KA. 1995. Unique adaptations of the metabolic biochemistry of tunas and billfishes for life in the pelagic environment. *Environ Biol Fishes* 42:65–97.
- Dobson GP, Wood SC, Daxboeck C, Perry SF. 1986. Intracellular buffering and oxygen transport in the Pacific blue marlin (*Makaira nigricans*): Adaptations to high-speed swimming. *Physiol Zool* 59:150–156.
- Donley JM, Dickson KA. 2000. Swimming kinematics of juvenile kawakawa tuna (*Euthynnus affinis*) and chub mackerel (*Scomber japonicus*). *J Exp Biol* 203:3103–3116.
- Dowis HJ, Sepulveda CA, Graham JB, Dickson KA. 2003. Swimming performance studies on the eastern Pacific bonito *Sarda chiliensis*, a close relative of the tunas (family Scombridae) II. Kinematics. *J Exp Biol* 206:2749–2758.
- Freadman MA. 1981. Swimming energetics of striped bass (*Morone saxatilis*) and bluefish (*Pomatomus saltatrix*): Hydrodynamic correlates of locomotion and gill ventilation. *J Exp Biol* 90:253–265.
- Graham JB. 2006. Aquatic and aerial respiration. In: Evans DH, Claiborne JB, editors. *The Physiology of Fishes*. 3rd ed. Boca Raton: CRC Press. pp 85–117.
- Graham JB, Dickson KA. 2000. The evolution of thunniform locomotion and heat conservation in scombrid fishes: New insights based on the morphology of *Allothunnus fallai*. *Zool J Linn Soc* 129:419–466.
- Graham JB, Dickson KA. 2001. Anatomical and physiological specializations for endothermy. In: Block BA, Stevens ED, editors. *Tuna: Physiology, Ecology and Evolution*. San Diego: Academic Press. pp 121–165.
- Gray IE. 1954. Comparative study of the gill area of marine fishes. *Biol Bull Mar Biol Lab Woods Hole* 107:219–225.
- Hughes GM. 1966. The dimensions of fish gills in relation to their function. *J Exp Biol* 45:177–195.
- Hughes GM. 1970. Morphological measurements on the gills of fishes in relation to their respiratory function. *Folia Morph* 18:78–95.
- Hughes GM. 1972. Morphometrics of fish gills. *Respir Physiol* 14:1–25.
- Hughes GM. 1984a. General anatomy of the gills. In: Hoar WS, Randall DJ, editors. *Fish Physiology*, Vol. 10A. Orlando: Academic Press. pp 1–72.
- Hughes GM. 1984b. Measurement of gill area in fishes: Practices and problems. *J Mar Biol Ass UK* 64:637–655.
- Hughes GM, Morgan M. 1973. The structure of fish gills in relation to their respiratory function. *Biol Rev* 48:419–475.
- Johnson GD. 1986. Scombroid phylogeny: An alternative hypothesis. *Bull Mar Sci* 39:1–41.
- Korsmeyer KE, Dewar H. 2001. Tuna metabolism and energetics. In: Block BA, Stevens ED, editors. *Tuna: Physiology, Ecology and Evolution*. San Diego: Academic Press. pp 35–78.
- Lauder GV. 1984. Pressure and water flow patterns in the respiratory tract of the bass (*Micropterus salmoides*). *J Exp Biol* 113:151–164.
- Magnuson JJ. 1978. Locomotion by scombrid fishes: Hydromechanics, morphology, and behavior. In: Hoar WS, Randall DJ, editors. *Fish Physiology*, Vol. 7. New York: Academic Press. pp 239–313.
- Mandic M, Todgham AE, Richards JG. 2009. Mechanisms and evolution of hypoxia tolerance in fish. *Proc R Soc B* 276:735–744.
- Muir BS. 1970. Contribution to the study of blood pathways in teleost gills. *Copeia* 1970:19–28.
- Muir BS, Brown CE. 1971. Effects of blood pathway on the blood-pressure drop in fish gills, with special reference to tunas. *J Fish Res Bd Can* 28:947–955.
- Muir BS, Hughes GM. 1969. Gill dimensions for three species of tunny. *J Exp Biol* 51:271–285.
- Muir BS, Kendall JI. 1968. Structural modifications in the gills of tunas and some other oceanic fishes. *Copeia* 1968:388–398.
- Olson KR, Dewar H, Graham JB, Brill RW. 2003. Vascular anatomy of the gills in a high energy demand teleost, the skipjack tuna (*Katsuwonus pelamis*). *J Exp Zool* 297A:17–31.
- Palzenberger M, Pohla H. 1992. Gill surface area of water-breathing freshwater fish. *Rev Fish Biol Fisheries* 2:187–196.
- Piiper J. 1971. Gill surface area: Fishes. In: Altman PL, Dittmer DS, editors. *Respiration and Circulation*. Bethesda, Maryland: Federation of American Societies for Experimental Biology. pp 119–121.
- Ponce-Díaz G, Ortega-García S, González-Ramírez PG. 1991. Analysis of sizes and weight-length relation of the striped marlin, *Tetrapturus audax* (Philippi, 1887) in Baja California Sur, Mexico. *Cien Mar* 17:69–82.
- Prince ED, Goodyear CP. 2006. Hypoxia-based habitat compression of tropical pelagic fishes. *Fish Oceanogr* 15:451–464.
- Roberts JL. 1975. Active branchial and ram gill ventilation in fishes. *Biol Bull Mar Biol Lab Woods Hole* 148:85–105.
- Roberts JL, Rowell DM. 1988. Periodic respiration of gill-breathing fishes. *Can J Zool* 66:182–190.
- Sepulveda C, Dickson KA. 2000. Maximum sustainable speeds and cost of swimming in juvenile kawakawa tuna (*Euthynnus affinis*) and chub mackerel (*Scomber japonicus*). *J Exp Biol* 203:3089–3101.
- Sepulveda CA, Dickson KA, Graham JB. 2003. Swimming performance studies on the eastern Pacific bonito *Sarda chiliensis*, a close relative of the tunas (family Scombridae) I. Energetics. *J Exp Biol* 206:2739–2748.
- Sepulveda CA, Knight A, Nasby-Lucas N, Domeier ML. Fine-scale movements of the swordfish (*Xiphias gladius*) in the Southern California Bight. *Fish Oceanogr* (in review).
- Steen JB, Berg T. 1966. The gills of two species of haemoglobin-free fishes compared to those of other teleosts, with a note on severe anaemia in an eel. *Comp Biochem Physiol* 18:517–526.
- Stevens ED, Lightfoot EN. 1986. Hydrodynamics of water flow in front of and through the gills of skipjack tuna. *Comp Biochem Physiol* 83A:255–259.
- Wegner NC, Sepulveda CA, Graham JB. 2006. Gill specializations in high-performance pelagic teleosts, with reference to striped marlin (*Tetrapturus audax*) and wahoo (*Acanthocybium solandri*). *Bull Mar Sci* 79:747–759.
- Westneat MW, Wainwright SA. 2001. Mechanical design for swimming: muscle, tendon, and bone. In: Block BA, Stevens ED, editors. *Tuna: Physiology, Ecology and Evolution*. San Diego: Academic Press. pp 271–311.